

Published in final edited form as:

Neuroscience. 2009 December 1; 164(2): 478–487. doi:10.1016/j.neuroscience.2009.08.049.

Expression of Wnt Receptors in Adult Spiral Ganglion Neurons: Frizzled 9 Localization at Growth Cones of Regenerating Neurites

S. M. Shah^{a,b,c}, Y.-J. Kang^{a,b,c}, B. L. Christensen^{a,c}, A. S. Feng^{a,b,c}, and R. Kollmar^{a,b,c,d,*}

^a Department of Molecular and Integrative Physiology, University of Illinois at Urbana-Champaign, Urbana, IL 61801, USA

^b Neuroscience Graduate Program, University of Illinois at Urbana-Champaign, Urbana, IL 61801, USA

^c Beckman Institute for Advanced Science and Technology, University of Illinois at Urbana-Champaign, Urbana, IL 61801, USA

Abstract

Little is known about signaling pathways, besides those of neurotrophic factors, that are operational in adult spiral ganglion neurons. In patients with sensorineural hearing loss, such pathways could eventually be targeted to stimulate and guide neurite outgrowth from the remnants of the spiral ganglion towards a cochlear implant, thereby improving the fidelity of sound transmission. To systematically identify neuronal receptors for guidance cues in the adult cochlea, we conducted a genome-wide cDNA microarray screen with two-month-old CBA/CaJ mice. A meta-analysis of our data and those from older mice in two other studies revealed the presence of neuronal transmembrane receptors that represent all four established guidance pathways—ephrin, netrin, semaphorin, and slit—in the mature cochlea as late as 15 months. In addition, we observed the expression of all known receptors for the Wnt morphogens, whose neuronal guidance function has only recently been recognized. *In situ* hybridizations located the mRNAs of the Wnt receptors frizzled 1, 4, 6, 9, and 10 specifically in adult spiral ganglion neurons. Finally, frizzled 9 protein was found in the growth cones of adult spiral ganglion neurons that were regenerating neurites in culture. We conclude from our results that adult spiral ganglion neurons are poised to respond to neurite damage, owing to the constitutive expression of a large and diverse collection of guidance receptors. Wnt signaling, in particular, emerges as a candidate pathway for guiding neurite outgrowth towards a cochlear implant after sensorineural hearing loss.

Keywords

Cell surface receptors; Cochlea; *In situ* hybridization; Mice; Microarray analysis

The cochlear implant is one of the most successful neural prostheses (Clark, 2003). It can initiate or restore hearing in patients with sensorineural deafness, which is commonly caused by noise, age, ototoxic drugs, or inherited mutations and is the most common sensory deficit

*Corresponding author: Department of Cell Biology, SUNY Downstate Medical Center, 450 Clarkson Ave., Box 5, Brooklyn, NY 11203, USA. Tel: x1-718-270-1014; fax: x1-718-270-3732. richard.kollmar@downstate.edu (R. Kollmar).

^dCurrent address: Department of Cell Biology, SUNY Downstate Medical Center, Brooklyn, NY 11203, USA.

Section Editor: Dr. Constantino Sotelo (Cellular Neuroscience)

Publisher's Disclaimer: This is a PDF file of an unedited manuscript that has been accepted for publication. As a service to our customers we are providing this early version of the manuscript. The manuscript will undergo copyediting, typesetting, and review of the resulting proof before it is published in its final citable form. Please note that during the production process errors may be discovered which could affect the content, and all legal disclaimers that apply to the journal pertain.

in developed countries among humans at any age (Gates and Mills, 2005; Smith et al., 2005). With current implant designs, however, the effective number of frequency bands is inadequate for conversing in a noisy environment, grasping tonal and prosodic elements of speech, or listening to music (Shannon, 2005). A major reason for this functional deficit is the current spread over the considerable distance between the electrodes implanted in the scala tympani and their targets, the somata of the spiral ganglion neurons in Rosenthal's canal. Minimizing this distance by promoting and guiding the growth of neurites towards the electrodes could reduce the electrical interference and substantially improve the quality of hearing (Wilson et al., 2003). This would be a major improvement for the increasing number of implantees who became deaf post-lingually and are used to a higher fidelity of sound reception (Zeng, 2004).

Sensorineural hearing loss characteristically results in the rapid degeneration of the neurites between the spiral ganglion and the organ of Corti because the sensory hair cells are damaged or missing and cannot provide trophic support (Spendlin, 1975; Gillespie and Shepherd, 2005). However, the somata and axonal projections to the brainstem can survive for many years (Nadol et al., 1989). Moreover, spontaneous, but sparse reinnervation of the organ of Corti has been observed in damaged animal cochleae *in vivo* (Lawner et al., 1997; Sugawara et al., 2005) as well as *in vitro* (Martinez-Monedero et al., 2006). Furthermore, neurites can regrow *in vitro* from the trunks of dissociated and cultured adult spiral ganglion neurons (Wei et al., 2007; reviewed in Vieira et al., 07). Together, these observations indicate that adult spiral ganglion neurons retain the capacity to regenerate neurites and that at least some guidance cues remain in place.

Studies of embryonic and early postnatal ear development suggest three principal groups of agents that might be used therapeutically to stimulate and guide neuritogenesis in the adult cochlea: First, neurotrophic factors—ciliary neurotrophic factor, leukemia inhibitory factor, brain derived neurotrophic factor, and neurotrophin 3, as well as fibroblast growth factors—can also exert tropic effects on spiral ganglion neurites (Rubel and Fritzschn, 2002; Gillespie and Shepherd, 2005). The last three factors have indeed been reported to promote neurite regeneration in the adult cochlea (Ernfors et al., 1996; Wise et al., 2005; Miller et al., 2007; Glueckert et al., 2008). Their expression patterns, though, suggest that neurotrophic factors are unlikely to choreograph the intricate pattern of cochlear innervation by themselves (Fritzschn et al., 2005). Second, members of each of the four established guidance-factor families—ephrins, netrins, semaphorins, and slits—have been detected in the developing cochlea (Webber and Raz, 2006; Fekete and Campero, 2007); a guidance function has been demonstrated so far only for Eph receptor A4 and netrin 1 *in vitro* (Brors et al., 2003; Lee and Warchol, 2008). Third, “wingless-related MMTV integration site” (Wnt) proteins are expressed throughout ear development at least until early postnatal stages (Daudet et al., 2002; Sienknecht and Fekete, 2008). Recently, these classic morphogens have also been recognized as guidance cues throughout the nervous system (Salinas and Zou, 2008). Wnts are attractive candidates for providing guidance in a labyrinthine organ like the cochlea because of their rich combinatorial repertoire of nineteen ligands, ten “frizzled homolog (Drosophila)” (*Fzd*) receptors plus “receptor-like tyrosine kinase” (*Ryk*), and three intracellular pathways (canonical, planar-cell polarity, and Wnt/Ca²⁺). To date, however, no systematic studies have been undertaken to determine which neuritogenic pathways, other than those of the neurotrophic factors, are operational in adult spiral ganglion neurons.

To identify receptors for guidance cues in the mature cochlea, we conducted a genome-wide cDNA microarray screen with modioli from adult mice. Furthermore, we investigated whether Wnt receptors are expressed in adult spiral ganglion neurons *in vivo* and are targeted to the growth cones of regenerating neurites *in vitro*. Based on our findings, we propose that manifold pathways related to neuritogenesis remain useable in the mature cochlea and that Wnt signaling

could be harnessed to stimulate and guide neurite outgrowth towards an implant in a damaged adult cochlea.

Experimental Procedures

Animals

Mice, strain CBA/CaJ (The Jackson Laboratory, Bar Harbor, ME), were maintained in our own colony. All experiments were conducted in accordance with protocols approved by the University of Illinois Institutional Animal Care and Use Committee.

Microarray hybridization

Animals were sacrificed at 8 weeks of age. From each cochlea, the modiolus containing the somata of the spiral ganglion neurons was dissected as cleanly as possible within 8 min, homogenized in Trizol (Invitrogen, Carlsbad, CA), and stored at -80°C . After purifying total RNA for each animal separately, its integrity was confirmed and its amount determined by capillary electrophoresis (2100 Bioanalyzer, Agilent Technologies, Santa Clara, CA). The six RNA samples were then linearly amplified and biotinylated with an Ovation Biotin kit (NuGEN, San Carlos, CA). The yields per animal of total RNA, amplified cDNA, and biotinylated and fragmented cDNA ranged from 8 to 21 ng, 5.2 to 6.4 μg , and 3.5 to 5.1 μg , respectively. Biotinylated cDNA from each animal was hybridized to a separate Mouse Expression Set 430 2.0 array (Affymetrix, Santa Clara, CA) and imaged at the Roy J. Carver Biotechnology Center of the University of Illinois at Urbana-Champaign. Statistical analyses were conducted with R software (version 2.8.1; R Development Core Team, 2008). The original cell intensities as well as descriptions of the pre-processing with Bioconductor tools (release 2.1; Gentleman et al., 2005), the probe-set selection on the basis of hybridization signal and Gene Ontology annotation (Ashburner et al., 2000), and the meta-analysis together with the data of Someya et al. (2007; 2008) have been deposited in the public Gene Expression Omnibus database (GEO; [http://www.ncbi.nlm.nih.gov/geo/Barrett et al., 2007](http://www.ncbi.nlm.nih.gov/geo/Barrett%20et%20al.,%202007)) under the accession GSE12810. For genes with more than multiple probe sets on the microarray, the one with the strongest hybridization signal was taken as representative.

Half the animals used for microarray hybridization and for real-time reverse transcription and polymerase chain reaction (RT-PCR; see below) had been exposed at four weeks of age to 5–20 kHz band-limited noise at 110 dB sound pressure level. After sacrifice one month later, however, we observed at best marginal differences in chronic gene-expression levels between the noise-exposed and unexposed groups (GEO entry GSE12810 and data not shown). The data from both groups were, therefore, pooled for the analyses presented here.

Reverse transcription and polymerase chain reaction

Oligonucleotide primers for RT-PCR were taken from the RTPriemerDB (Pattyn et al., 2006) and PrimerBank (Wang and Seed, 2003) databases or designed with Primer3 software (Rozen and Skaletsky, 2000; see Table 1). Total RNA was isolated from two-month-old modioli as above, treated with DNase (Turbo DNA-free kit; Ambion), and quantitated by fluorometry. First-strand cDNA was synthesized from equal amounts of RNA at 50°C with oligo(dT)₁₈, RNase inhibitor (SuperaseIn; Ambion), and reverse transcriptase (Superscript III; Invitrogen). For mock cDNA synthesis, the reverse transcriptase was heat-inactivated at 90°C for 5 min beforehand, and the reaction was frozen immediately after assembly.

For qualitative assays, the amplification reactions included Taq DNA polymerase (Invitrogen), 0.2 μM of each primer (Table 1), and pooled cDNA corresponding to 1 ng/ μl of RNA; after 30 cycles with an annealing temperature of 55°C , the products were analyzed by agarose-gel electrophoresis. The DNase treatment and mock cDNA synthesis were included to ensure that

the PCR products were derived from mRNA and not genomic DNA, since most *Fzd* genes lack introns. In addition, the findings were replicated independently by another experimenter with a new set of reagents in a separate building.

For real-time assays, the reactions comprised a reagent blend (iQ SYBR Green Supermix; Biorad, Hercules, CA), 0.4 μM of each primer (Table 1), and cDNA from individual mice corresponding to 0.2 ng/ μl of RNA. They were denatured at 95°C for 3 min, followed by 45 cycles of denaturation at 95°C, annealing at 55°C, and extension at 72°C for 30 s each (iCycler iQ; Biorad). The fluorescence signal was specific, since neither primer dimers nor products of the wrong size were detected on melting curves and agarose gels. A common threshold signal was chosen manually in the linear amplification range of all samples by inspecting the log-transformed fluorescence plotted against the cycle number (iCycler iQ Optical System Software, Version 3.0a; BioRad).

In situ hybridization

Partial mouse *Fzd* and *Ryk* cDNAs were amplified in RT-PCRs with the primers shown in Table 1 and cloned into the vector pBluescript II SK (+) (Stratagene, La Jolla, CA). Digoxigenin-labeled riboprobes were synthesized from these templates as described (Kang et al., 2008); their concentration and integrity were confirmed by dot blotting and by gel electrophoresis and antibody detection after membrane transfer. Two-month-old cochleae were fixed by immersion in 4% wt/vol paraformaldehyde in phosphate-buffered saline at 4°C overnight, decalcified in 0.5 M EDTA (pH 7.0) at 4°C for three days, and embedded in paraffin (Paraplast Plus; SPI Supplies, West Chester, PA). Longitudinal 6 μm -thick sections were mounted on positively-charged slides (Superfrost Plus; Fisher Scientific, Pittsburgh, PA) and hybridized to detect mRNAs as described (Acloque et al., 2008). Some sections were stained with hematoxylin and eosin instead. Tiled images were stitched together with Axiovision software (release 4.5; Carl Zeiss, Thornwood, NY). Contrast was adjusted to match the dynamic range of the digital images with Photoshop software (version 8.0; Adobe, San Jose, CA).

Immunofluorescence microscopy

Adult spiral ganglion neurons were cultured in chambered glass slides (Lab-Tek; Nalge Nunc, Rochester, NY) and labeled for immunofluorescence detection with the nuclear stain 0.3 μM 4',6-diamidino-2-phenylindole (DAPI; Molecular Probes, Eugene, OR), 2 $\mu\text{g}/\text{ml}$ Alexa-488-conjugated monoclonal mouse antibody against the neuronal marker $\beta\text{III-tubulin}$ (TUBB3; Covance, Princeton, NJ), 5 $\mu\text{g}/\text{ml}$ affinity-purified polyclonal rabbit antibodies against human and mouse FZD9 protein (ab13000; Abcam, Cambridge, MA), and 7.5 $\mu\text{g}/\text{ml}$ rhodamine-conjugated donkey anti-rabbit-IgG antibodies (Jackson ImmunoResearch Laboratories, West Grove, PA) as described (Vieira et al., 2007). As a negative control, the antibodies against FZD9 were omitted or replaced with purified normal rabbit IgG (Jackson) at the same concentration. The digital images were processed as above for *in situ* hybridization.

Results

Manifold neuronal receptors expressed in the adult cochlea

To determine which potential guidance receptors were present in the adult cochlea, we conducted a microarray hybridization screen with dissected modiolis from six 8-week-old CBA/CaJ mice. First, we sought to establish a rational criterion to discern expressed genes. The probability density plot of the hybridization signals for all 45,101 probe-sets and all six mice suggested two slightly overlapping probe-set distributions (Fig. 1): The first was narrow and almost symmetrical, with a center near the low end of the range; the second was broad and skewed, with a long tail towards the high end of the range. Because the former represented

most likely probe sets with background hybridization signals, we chose the crossover point of the two distribution functions, the 44th percentile, as the cutoff for true expression in our further analyses.

Next, we looked for evidence of robust expression of potential guidance receptors. For increased statistical power, we focused our analysis on 1,369 probe sets representing 738 genes with a Gene Ontology annotation as neuronal transmembrane receptors. In addition, we combined our modiolus data with those from the untreated control mice in two studies that had used the same microarray platform to measure differential gene expression in older cochleae (Someya et al., 2007; Someya et al., 2008). The Pearson coefficient for all hybridization signals between the three data series ranged from 0.55 to 0.87, indicating that there was a significant correlation ($P \leq 5 \cdot 10^{-4}$) despite the differences in age, strain, and sample preparation and that a meta-analysis was legitimate. In the pooled data from all 17 mice, 339 of the 1,369 probe sets for neuronal transmembrane receptors representing 242 unique genes exhibited a mean hybridization signal that was significantly higher than the 44th-percentile cutoff ($P < 0.05$ after Bonferroni correction in one-sided t tests); another 300 probe sets, including 177 more unique genes, exhibited a mean hybridization signal that was higher than, but not significantly different from the cutoff (Supplemental Table 1). Similar results were obtained when our hybridization data were analyzed alone. All four established guidance-factor pathways were represented among the expressed genes (Table 2). Likewise, all eleven Wnt receptors were present—*Fzd1* to *Fzd10* and *Ryk*—as well as two co-receptors. In addition, most receptors for neurotrophic factors were detected (see Supplemental Table 1). We concluded from the results of our exploratory microarray screen and meta-analysis that an ample repertoire of neuronal signaling pathways is available in the adult cochlea.

Five Fzd genes expressed in adult spiral ganglion neurons

To confirm and extend our microarray findings, we concentrated on the Wnt pathway, whose involvement in cochlear neuritogenesis had not been investigated previously. First, we qualitatively confirmed the presence of the *Fzd1* to *Fzd10* and *Ryk* mRNAs by using the RT-PCR as an independent method. Products of the expected size were amplified for all eleven genes from a template of modiolar RNA subjected to cDNA synthesis (Fig. 2). This result was consistent with our observation of microarray signals above the cutoff for all eleven Wnt receptors.

Next, we conducted *in situ* hybridizations to determine which, if any, of the *Fzd* and *Ryk* genes were expressed in spiral ganglion neurons. On longitudinal sections of cochleae from 6-to-8-week-old mice, antisense riboprobes for *Fzd1*, *-4*, *-6*, *-9*, and *-10* specifically labeled the somata of spiral ganglion neurons in Rosenthal's canal (Fig. 3). Intriguingly, the labeling in the cochlea decreased from the apical to the basal turns for *Fzd1*, *-4*, and *-10*, suggesting a gradient of expression along the cochlea's tonotopic map. The antisense *Fzd6* probe also bound to most cells in the saccular macula and to neurons in Scarpa's ganglion next to the cochlea's base (Fig. 4).

Finally, we quantified the abundance of Wnt receptor mRNAs in the modiolus by performing real-time RT-PCRs. Some of the *Fzd* genes that had not exhibited specific labeling of spiral ganglion neurons (Fig. 3) were omitted from the experiment. The mean mRNA levels across 12 nine-week-old mice, as measured individually by real-time RT-PCR, correlated strongly with those measured before by microarray hybridization (Fig. 5). The results of these gene-specific experiments lend strong support to our genome-wide assessment of guidance-receptor expression in the cochlea. Furthermore, they demonstrate that adult spiral ganglion express up to five different Wnt receptors at a robust level.

FZD9 protein targeted to growth cones of regenerating spiral ganglion neurons

Finally, we employed immunofluorescence microscopy to examine whether spiral ganglion neurons sport Wnt receptors at sites of neurite regrowth. We used antibodies against FZD9, whose cognate mRNA had been detected in all of our microarray, RT-PCR, and *in situ* hybridization analyses (see above). Spiral ganglion neurons from adult mice were dissociated, and their trunks allowed to regrow neurites in serum-free culture as an *in vitro* model of regeneration. Immunofluorescence microscopy located FZD9 specifically in all neurons, in particular at the growth cones, regardless of the number and the length of neurites (Fig. 6A–C and G–I). Qualitatively, the FZD9 fluorescence appeared to be stronger in spindle-shaped “simple” growth cones than in branched “complex” growth cones. This result was consistent with the detection of *Fzd9* mRNA from apex to base and demonstrated that FZD9 occurs in the right place to modulate and guide neurite regeneration in adult spiral ganglion neurons.

Discussion

Our results show that a large and diverse collection of neuronal transmembrane receptors representing all four established guidance pathways—ephrin, netrin, semaphorin, and slit—is present in the adult mouse cochlea. We also observed expression of all Wnt receptors and located the mRNAs of *Fzd1*, *-4*, *-6*, *-9*, and *-10* specifically in adult spiral ganglion neurons. Finally, we detected FZD9 protein in the growth cones of adult spiral ganglion neurons that were regenerating neurites in culture.

The detection of dozens of guidance receptors in the adult cochlea as late as 15 months may come as a surprise. After all, the innervation of the murine organ of Corti is complete by the time hearing commences on postnatal day 10 (P10; Huang et al., 2007). Previous studies of global gene expression in the adult cochlea have published in general only small excerpts of their primary data and not focused on neuronal receptors as a group. We closed this gap by combining our own data from the modiolus of two-month-old mice with two data sets in the public GEO database from the cochleae of four- to fifteen-month-old mice that had been collected on the same microarray platform (Someya et al., 2007; Someya et al., 2008). The hybridization signals for neuronal receptors in these three independent data sets were in close agreement. Furthermore, the signals corresponded well with our RT-PCR results for all eleven Wnt receptors and five other test genes, which covered a wide range of mRNA levels. In addition, the results of our meta-analysis were largely consistent with microarray data from one-month-old CBA/CAJ mice by Chen and Corey (2002; see Table 2). Finally, expression of assorted guidance receptors in the adult cochlea or specifically in spiral ganglion neurons has been demonstrated in several studies that employed RT-PCR or immunocytochemistry (see Table 2). Taken together, these concordances indicate that our microarray results faithfully represent the expression of neuronal transmembrane receptors in the adult cochlea.

The expression of specific *Fzd* genes in adult spiral ganglion neurons is a continuation of the pattern reported previously for the embryonic ganglion and the early postnatal cochlea. In the developing ear, the Wnt pathway functions in otic induction (Ohyama et al., 2007), axis and boundary specification (Bok et al., 2007), the regulation of planar cell polarity, particularly in hair cells (Montcouquiol et al., 2006a), and vascularization, with the atypical norrin ligand (Xu et al., 2004). Accordingly, numerous *Fzd* genes have been found to be expressed throughout the embryonic and early postnatal ear (Wang et al., 2001; Stevens et al., 2003; Visel et al., 2004; Xu et al., 2004; Montcouquiol et al., 2006b; Wang et al., 2006; Sajan et al., 2007). The latest stages investigated have been P14 in the rat, with *Fzd1* to *-4*, *-6*, *-9*, detected in the cochlea by RT-PCR (Daudet et al., 2002). The auditory ganglion is mentioned only by Sienknecht and Fekete in their thorough study of the chicken’s developing cochlear duct (2008): strong expression for *Fzd1* and *-9*; moderate for *Fzd2*, *-4*, *-7*, and *-8*; and none for *Fzd10*. Allowing for inter-species differences, the latter two reports agree well with our

findings of *Fzd1*, *-4*, *-6*, *-9*, and weak *-10* expression in spiral ganglion neurons of the adult mouse.

What roles might the neuronal receptors play in the adult cochlea? For most of the classic guidance receptors, the cellular location has not been ascertained, and their cognate pathways participate in a wide range of developmental and homeostatic processes outside the nervous system (Hinck, 2004). Nevertheless, at least some of the ephrin, netrin, semaphorin, and slit receptors may provide guidance to spiral ganglion neurons, as evidenced by the responsiveness of cultured neurons from mice at P28 to P35 to netrin 1 (Lee and Warchol, 2008).

For *Fzd1*, *-4*, *-6*, *-9*, and *-10*, the selective expression in adult spiral ganglion neurons shown here also suggests roles related to neuritogenesis and synapse formation, as documented elsewhere in the nervous system (Salinas and Zou, 2008), rather than to the classic morphogenetic processes during ear development. (We cannot speak to the other Wnt receptors, as we could not locate them in our *in situ* hybridizations.) Our detection of FZD9 protein in the growth cones of regenerating neurites *in vitro* is consistent with this hypothesis, but its presence in adult growth cones *in vivo* remains to be demonstrated. Further support comes from the complementary localization of the Wnts themselves, although systematic studies have been conducted only at embryonic and postnatal stages of development: In the chicken embryo, *Wnt4*, *-5a*, *-5b*, *-7a*, *-7b*, *-9a*, and *-11*, as well as the Wnt inhibitors “secreted frizzled-related protein” 2 and 3, are expressed mostly in non-sensory domains that extend along the cochlea’s long axis (Sienknecht and Fekete, 2008). In the rat cochlea at P14 and P21, *Wnt4*, *-5b*, and *-7a* expression has been located in domains that surround the neurites and somata; *Wnt7a* mRNA has also been located in spiral ganglion neurons and outer hair cells (Daudet et al., 2002). Chen and Corey in the analysis of their microarray data have pointed out a prevalence of *Wnt4*, *-5a*, *-5b*, and *-7b* expression in mouse cochleae at P32 (2002), and our preliminary RT-PCR experiments have detected a similar set of *Wnt* mRNAs in two-month-old animals (S.M. Shah, unpublished observations). Since Wnts do not seem to be secreted from inner hair cells, the targets of the spiral ganglion neurons, their presumptive guidance role may be mostly repulsive, keeping neurites from straying from their path to the organ of Corti.

The Wnts in the cochlea most likely join forces with other signaling factors, as they do elsewhere in the nervous system; for example, WNT3 regulates the arborization of neurotrophin-3-responsive sensory neurons in the spinal cord (Krylova et al., 2002), and parallel gradients of WNT3/RYK and EFN1/EPHB ligand/receptor pairs control the topographic mapping of retinotectal projections (Schmitt et al., 2006). The plenitude of possible Wnt ligand-receptor combinations also leaves room for other roles, such as guidance of the axonal projections from the spiral ganglion to the brainstem (Rubel and Fritzsche, 2002) and control of neuronal survival and death (Ille and Sommer, 2005). We therefore propose that stable complements of both Wnt and frizzled proteins are present in the cochlea from embryonic to adult stages and provide guidance cues to the spiral ganglion neurons for neurite outgrowth, maintenance, and regeneration in conjunction with other neurotrophic and neurotropic signals.

Our finding of a large number of known and potential guidance receptors in the adult cochlea suggests that its neurons are not static and are poised to respond to damage. Functional experiments *in vitro* and *in vivo* will show whether the established guidance pathways as well as Wnt signaling can be harnessed to augment neurotrophic treatments and promote and guide the regeneration of damaged neurites after sensorineural hearing loss.

Supplementary Material

Refer to Web version on PubMed Central for supplementary material.

Acknowledgments

We thank Dr. Steven Clough for the use of his Agilent Bioanalyzer, Dr. Mark Band for advice on microarray hybridizations, Dr. Shinichi Someya and colleagues for making their microarray data publicly available, Drs. Zheng-Yi Chen and David Corey for sharing their microarray data, Dr. Lori Raetzman for advice on and Mr. Chirag Patel for assistance with *in situ* hybridizations, and Ms. Amy Stevenson for comments on the manuscript. This work was supported by training grant T32 DC006612 from the National Institute on Deafness and Other Communication Disorders and a medical student training grant from the American Otological Society to S.M.S., by grants from the Campus Research Board and the Mary Jane Neer Fund at the University of Illinois to A.S.F., and by University of Illinois start-up funds and a research award from the National Organization for Hearing Research to R.K.

Abbreviations

| | |
|---------------|---|
| EfnB1 | ephrin B1 |
| Ephb | Eph receptor B |
| Fzd | frizzled homolog (<i>Drosophila</i>) |
| GEO | Gene Expression Omnibus |
| P10 | postnatal day 10 |
| RT-PCR | reverse transcription and polymerase chain reaction |
| Ryk | receptor-like tyrosine kinase |
| TUBB3 | β III-tubulin protein |
| Wnt | wingless-related MMTV integration site |

References

- Acloque H, Wilkinson DG, Nieto MA. In situ hybridization analysis of chick embryos in whole-mount and tissue sections. *Methods Cell Biol* 2008;87:169–185. [PubMed: 18485297]
- Ashburner M, Ball CA, Blake JA, Botstein D, Butler H, Cherry JM, Davis AP, Dolinski K, Dwight SS, Eppig JT, Harris MA, Hill DP, Issel-Tarver L, Kasarskis A, Lewis S, Matese JC, Richardson JE, Ringwald M, Rubin GM, Sherlock G. Gene ontology: tool for the unification of biology. The Gene Ontology Consortium. *Nat Genet* 2000;25:25–29. [PubMed: 10802651]
- Barrett T, Troup DB, Wilhite SE, Ledoux P, Rudnev D, Evangelista C, Kim IF, Soboleva A, Tomashevsky M, Edgar R. NCBI GEO: mining tens of millions of expression profiles--database and tools update. *Nucleic Acids Res* 2007;35:D760–5. [PubMed: 17099226]
- Bianchi LM, Dinsio K, Davoli K, Gale NW. Lac z Histochemistry and immunohistochemistry reveal ephrin-B ligand expression in the inner ear. *J Histochem Cytochem* 2002;50:1641–1645. [PubMed: 12486086]

- Bianchi LM, Gale NW. Distribution of Eph-related molecules in the developing and mature cochlea. *Hear Res* 1998;117:161–172. [PubMed: 9557986]
- Bianchi LM, Liu H. Comparison of ephrin-A ligand and EphA receptor distribution in the developing inner ear. *Anat Rec* 1999;254:127–134. [PubMed: 9892426]
- Bok J, Chang W, Wu DK. Patterning and morphogenesis of the vertebrate inner ear. *Int J Dev Biol* 2007;51:521–533. [PubMed: 17891714]
- Brors D, Bodmer D, Pak K, Aletsee C, Schafers M, Dazert S, Ryan AF. EphA4 provides repulsive signals to developing cochlear ganglion neurites mediated through ephrin-B2 and -B3. *J Comp Neurol* 2003;462:90–100. [PubMed: 12761826]
- Chen ZY, Corey DP. An inner ear gene expression database. *J Assoc Res Otolaryngol* 2002;3:140–148. [PubMed: 12162364]
- Clark, G. *Cochlear Implants: Fundamentals and Applications*. New York: Springer; 2003.
- Daudet N, Ripoll C, Moles JP, Rebillard G. Expression of members of Wnt and Frizzled gene families in the postnatal rat cochlea. *Brain Res Mol Brain Res* 2002;105:98–107. [PubMed: 12399112]
- Ernfors P, Duan ML, ElShamy WM, Canlon B. Protection of auditory neurons from aminoglycoside toxicity by neurotrophin-3. *Nat Med* 1996;2:463–467. [PubMed: 8597959]
- Fekete DM, Campero AM. Axon guidance in the inner ear. *Int J Dev Biol* 2007;51:549–556. [PubMed: 17891716]
- Fritzsch B, Pauley S, Matei V, Katz DM, Xiang M, Tessarollo L. Mutant mice reveal the molecular and cellular basis for specific sensory connections to inner ear epithelia and primary nuclei of the brain. *Hear Res* 2005;206:52–63. [PubMed: 16080998]
- Gates GA, Mills JH. Presbycusis. *Lancet* 2005;366:1111–1120. [PubMed: 16182900]
- Gentleman, R.; Carey, V.; Huber, W.; Irizarry, R.; Dudoit, S. *Bioinformatics and Computational Biology Solutions Using R and Bioconductor*. New York: Springer; 2005.
- Gillespie LN, Shepherd RK. Clinical application of neurotrophic factors: the potential for primary auditory neuron protection. *Eur J Neurosci* 2005;22:2123–2133. [PubMed: 16262651]
- Glueckert R, Bitsche M, Miller JM, Zhu Y, Prieskorn DM, Altschuler RA, Schrott-Fischer A. Deafferentation-associated changes in afferent and efferent processes in the guinea pig cochlea and afferent regeneration with chronic intrascalar brain-derived neurotrophic factor and acidic fibroblast growth factor. *J Comp Neurol* 2008;507:1602–1621. [PubMed: 18220258]
- Hinck L. The versatile roles of “axon guidance” cues in tissue morphogenesis. *Dev Cell* 2004;7:783–793. [PubMed: 15572123]
- Howard MA, Rodenas-Ruano A, Henkemeyer M, Martin GK, Lonsbury-Martin BL, Liebl DJ. Eph receptor deficiencies lead to altered cochlear function. *Hear Res* 2003;178:118–130. [PubMed: 12684184]
- Huang LC, Thorne PR, Housley GD, Montgomery JM. Spatiotemporal definition of neurite outgrowth, refinement and retraction in the developing mouse cochlea. *Development* 2007;134:2925–2933. [PubMed: 17626062]
- Ille F, Sommer L. Wnt signaling: multiple functions in neural development. *Cell Mol Life Sci* 2005;62:1100–1108. [PubMed: 15928805]
- Kang YJ, Stevenson AK, Yau PM, Kollmar R. Sparc protein is required for normal growth of zebrafish otoliths. *J Assoc Res Otolaryngol* 2008;9:436–451. [PubMed: 18784957]
- Krylova O, Herreros J, Cleverley KE, Ehler E, Henriquez JP, Hughes SM, Salinas PC. WNT-3, expressed by motoneurons, regulates terminal arborization of neurotrophin-3-responsive spinal sensory neurons. *Neuron* 2002;35:1043–1056. [PubMed: 12354395]
- Lawner BE, Harding GW, Bohne BA. Time course of nerve-fiber regeneration in the noise-damaged mammalian cochlea. *Int J Dev Neurosci* 1997;15:601–617. [PubMed: 9263037]
- Lee KH, Warchol ME. Promotion of neurite outgrowth and axon guidance in spiral ganglion cells by netrin-1. *Arch Otolaryngol Head Neck Surg* 2008;134:146–151. [PubMed: 18283156]
- Martinez-Monedero R, Corrales CE, Cuajungco MP, Heller S, Edge AS. Reinnervation of hair cells by auditory neurons after selective removal of spiral ganglion neurons. *J Neurobiol* 2006;66:319–331. [PubMed: 16408287]

- Miller JM, Le Prell CG, Prieskorn DM, Wys NL, Altschuler RA. Delayed neurotrophin treatment following deafness rescues spiral ganglion cells from death and promotes regrowth of auditory nerve peripheral processes: Effects of brain-derived neurotrophic factor and fibroblast growth factor. *J Neurosci Res* 2007;85:1959–1969. [PubMed: 17492794]
- Montcouquiol M, Crenshaw EB, Kelley MW. Noncanonical Wnt signaling and neural polarity. *Annu Rev Neurosci* 2006a;29:363–386. [PubMed: 16776590]
- Montcouquiol M, Sans N, Huss D, Kach J, Dickman JD, Forge A, Rachel RA, Copeland NG, Jenkins NA, Bogani D, Murdoch J, Warchol ME, Wenthold RJ, Kelley MW. Asymmetric localization of Vangl2 and Fz3 indicate novel mechanisms for planar cell polarity in mammals. *J Neurosci* 2006b;26:5265–5275. [PubMed: 16687519]
- Nadol JB Jr, Young YS, Glynn RJ. Survival of spiral ganglion cells in profound sensorineural hearing loss: implications for cochlear implantation. *Ann Otol Rhinol Laryngol* 1989;98:411–416. [PubMed: 2729822]
- Ohyama T, Groves AK, Martin K. The first steps towards hearing: mechanisms of otic placode induction. *Int J Dev Biol* 2007;51:463–472. [PubMed: 17891709]
- Pattyn F, Robbrecht P, De Paep A, Speleman F, Vandesompele J. RTPrimerDB: the real-time PCR primer and probe database, major update 2006. *Nucleic Acids Res* 2006;34:D684–8. [PubMed: 16381959]
- R Development Core Team. R: A Language and Environment for Statistical Computing. Vienna, Austria: R Foundation for Statistical Computing; 2008.
- Rozen S, Skaletsky H. Primer3 on the WWW for general users and for biologist programmers. *Methods Mol Biol* 2000;132:365–386. [PubMed: 10547847]
- Rubel EW, Fritsch B. Auditory system development: primary auditory neurons and their targets. *Annu Rev Neurosci* 2002;25:51–101. [PubMed: 12052904]
- Sajan SA, Warchol ME, Lovett M. Toward a systems biology of mouse inner ear organogenesis: gene expression pathways, patterns and network analysis. *Genetics* 2007;177:631–653. [PubMed: 17660535]
- Salinas PC, Zou Y. Wnt signaling in neural circuit assembly. *Annu Rev Neurosci* 2008;31:339–358. [PubMed: 18558859]
- Schmitt AM, Shi J, Wolf AM, Lu CC, King LA, Zou Y. Wnt-Ryk signalling mediates medial-lateral retinotectal topographic mapping. *Nature* 2006;439:31–37. [PubMed: 16280981]
- Shannon RV. Speech and music have different requirements for spectral resolution. *Int Rev Neurobiol* 2005;70:121–134. [PubMed: 16472633]
- Sienknecht UJ, Fekete DM. Comprehensive Wnt-related gene expression during cochlear duct development in chicken. *J Comp Neurol* 2008;510:378–395. [PubMed: 18671253]
- Smith RJ, Bale JF Jr, White KR. Sensorineural hearing loss in children. *Lancet* 2005;365:879–890. [PubMed: 15752533]
- Someya S, Yamasoba T, Kujoth GC, Pugh TD, Weindruch R, Tanokura M, Prolla TA. The role of mtDNA mutations in the pathogenesis of age-related hearing loss in mice carrying a mutator DNA polymerase gamma. *Neurobiol Aging* 2008;29:1080–1092. [PubMed: 17363114]
- Someya S, Yamasoba T, Weindruch R, Prolla TA, Tanokura M. Caloric restriction suppresses apoptotic cell death in the mammalian cochlea and leads to prevention of presbycusis. *Neurobiol Aging* 2007;28:1613–1622. [PubMed: 16890326]
- Spoendlin H. Retrograde degeneration of the cochlear nerve. *Acta Otolaryngol* 1975;79:266–275. [PubMed: 1094788]
- Stevens CB, Davies AL, Battista S, Lewis JH, Fekete DM. Forced activation of Wnt signaling alters morphogenesis and sensory organ identity in the chicken inner ear. *Dev Biol* 2003;261:149–164. [PubMed: 12941626]
- Sugawara M, Corfas G, Liberman MC. Influence of supporting cells on neuronal degeneration after hair cell loss. *J Assoc Res Otolaryngol* 2005;6:136–147. [PubMed: 15952050]
- Vieira M, Christensen BL, Wheeler BC, Feng AS, Kollmar R. Survival and stimulation of neurite outgrowth in a serum-free culture of spiral ganglion neurons from adult mice. *Hear Res* 2007;230:17–23. [PubMed: 17521837]

- Visel A, Thaller C, Eichele G. GenePaint.org: an atlas of gene expression patterns in the mouse embryo. *Nucleic Acids Res* 2004;32:D552–6. [PubMed: 14681479]
- Wang X, Seed B. A PCR primer bank for quantitative gene expression analysis. *Nucleic Acids Res* 2003;31:e154. [PubMed: 14654707]
- Wang Y, Guo N, Nathans J. The role of Frizzled3 and Frizzled6 in neural tube closure and in the planar polarity of inner-ear sensory hair cells. *J Neurosci* 2006;26:2147–2156. [PubMed: 16495441]
- Wang Y, Huso D, Cahill H, Ryugo D, Nathans J. Progressive cerebellar, auditory, and esophageal dysfunction caused by targeted disruption of the frizzled-4 gene. *J Neurosci* 2001;21:4761–4771. [PubMed: 11425903]
- Webber A, Raz Y. Axon guidance cues in auditory development. *Anat Rec A Discov Mol Cell Evol Biol* 2006;288:390–396. [PubMed: 16550548]
- Wei D, Jin Z, Järlebark L, Scarfone E, Ulfendahl M. Survival, synaptogenesis, and regeneration of adult mouse spiral ganglion neurons in vitro. *Dev Neurobiol* 2007;67:108–122. [PubMed: 17443776]
- Wilson BS, Lawson DT, Muller JM, Tyler RS, Kiefer J. Cochlear implants: some likely next steps. *Annu Rev Biomed Eng* 2003;5:207–249. [PubMed: 12704085]
- Wise AK, Richardson R, Hardman J, Clark G, O’leary S. Resprouting and survival of guinea pig cochlear neurons in response to the administration of the neurotrophins brain-derived neurotrophic factor and neurotrophin-3. *J Comp Neurol* 2005;487:147–165. [PubMed: 15880560]
- Xu Q, Wang Y, Dabdoub A, Smallwood PM, Williams J, Woods C, Kelley MW, Jiang L, Tasman W, Zhang K, Nathans J. Vascular development in the retina and inner ear: control by Norrin and Frizzled-4, a high-affinity ligand-receptor pair. *Cell* 2004;116:883–895. [PubMed: 15035989]
- Zeng FG. Trends in cochlear implants. *Trends Amplif* 2004;8:1–34. [PubMed: 15247993]

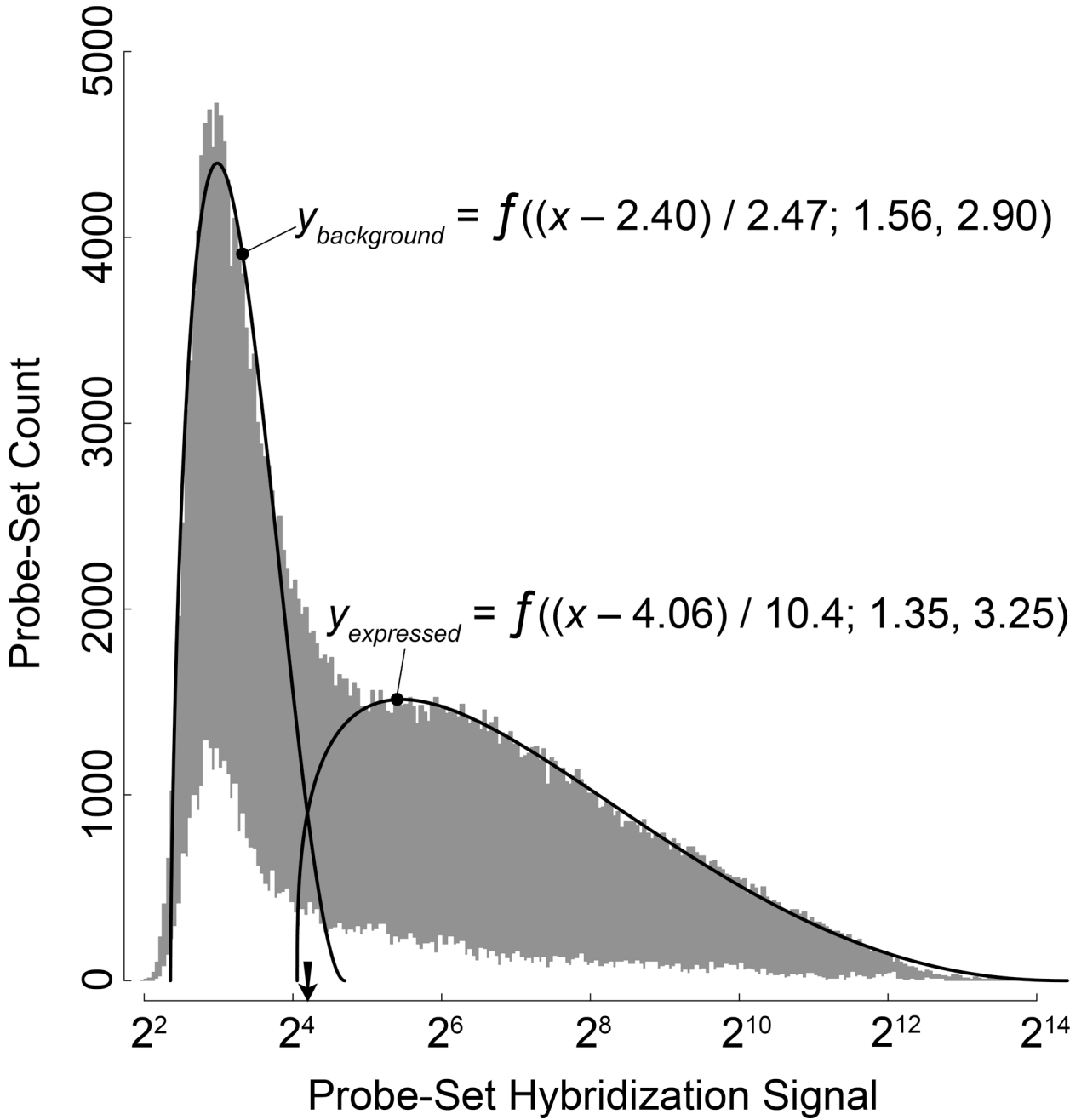


Fig. 1. Establishing a cutoff criterion for true expression versus background

Density distribution of the mean \log_2 -transformed hybridization signals for all six mice (GEO accession GSE12810). Gray histogram, all 45,105 probe sets on the mouse 430 2.0 microarray; white histogram, the 1,369 probe sets annotated as neuronal transmembrane receptors, with fivefold-magnified ordinate. Solid lines, beta distributions $f(x'; \alpha, \beta)$ fitted to the gray histogram with $x' = (x - \text{offset}) / \text{scale factor}$. Arrow, the crossover of the fitted lines at a hybridization signal of $2^{4.25}$ corresponding to the 44th-percentile cutoff.

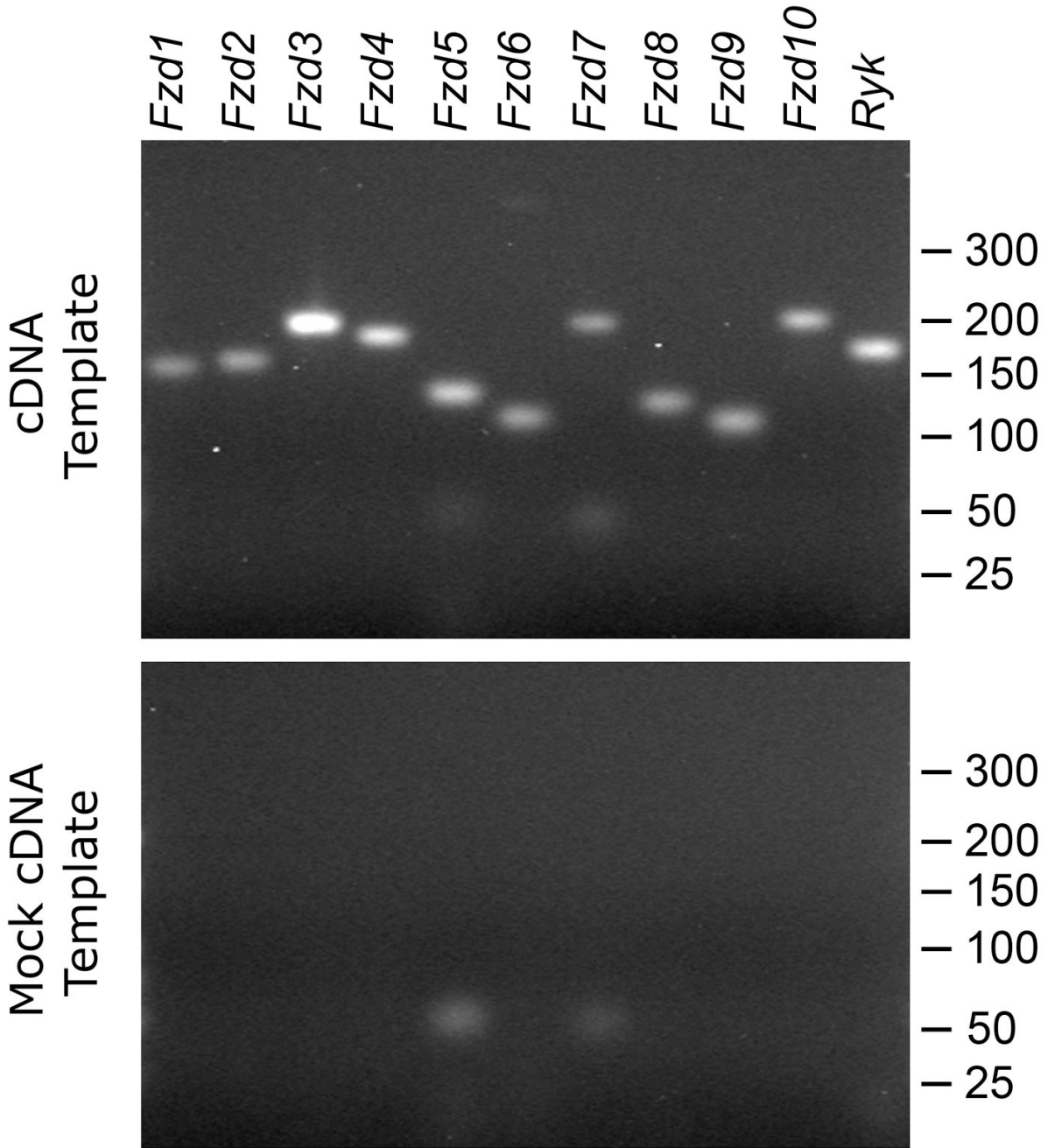


Fig. 2. Expression of all Wnt receptors in the modiolus of adult mice

(Top) The mRNAs of *Fzd1* to *Fzd10* and *Ryk* were detected in qualitative RT-PCRs with a cDNA template derived from two-month-old mice (see Table 1 for expected product sizes). (Bottom) No products were amplified from a mock cDNA template synthesized after heat-inactivating the reverse transcriptase. Marker sizes in base pairs indicated on the right.

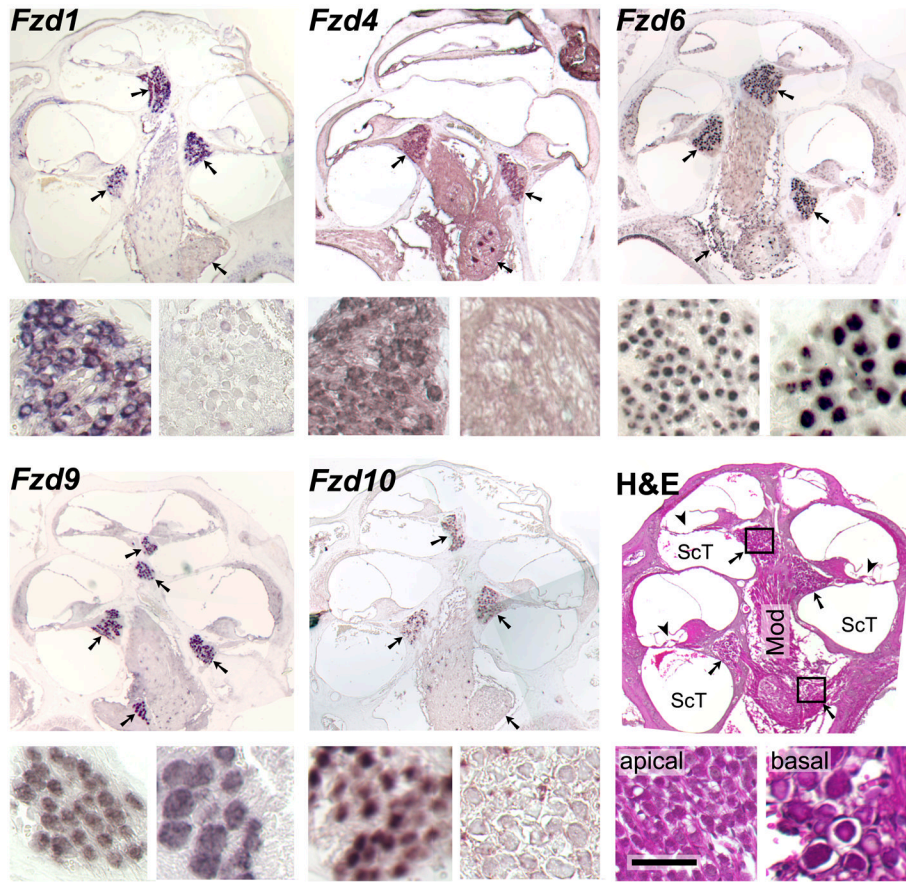


Fig. 3. Selective expression of Wnt receptors in adult spiral ganglion neurons
In situ hybridizations of antisense riboprobes for the indicated mRNAs to longitudinal paraffin sections of cochleae from two-month old mice, with the apex at the top. Arrows point at the cross-sections of the spiral ganglion inside Rosenthal's canal; note that some cross sections lack the brown or purple hybridization signal. The smaller panels at the bottom-left and -right of each triad show details from the apical- and basal-most cross sections, respectively, as indicated for the sample stained with hematoxylin and eosin (H&E). Antisense probes for the remaining six Wnt receptors did not exhibit specific labeling, nor did any of the sense probes (data not shown). Mod, modiolus; ScT, scala tympani; arrowheads, location of the organ of Corti with hair cells; scale bar, 300 μ m for the large and 50 μ m for the small panels.

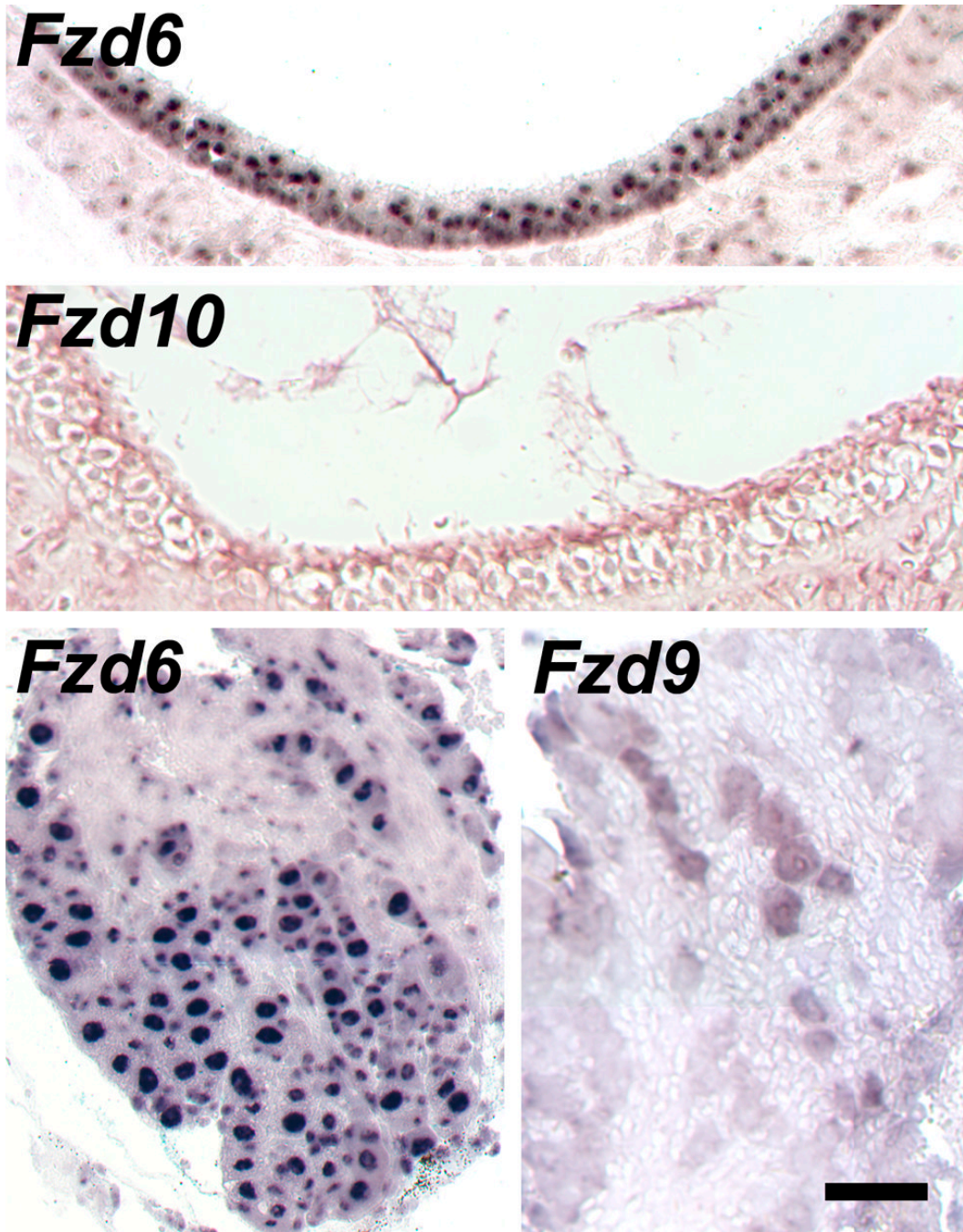


Fig. 4. Expression of *Fzd6* in the adult vestibular periphery

In situ hybridizations of antisense riboprobes for the indicated *Fzd* mRNAs to paraffin sections from two-month old mice. Top two panels, cross-sections of the saccular sensory macula; bottom two panels, Scarpa's ganglion of the vestibular nerve. No labeling was observed for the other Wnt receptors, as exemplified for *Fzd9* and *-10*, or with sense probes. Scale bar, 40 μ m for the top and 50 μ m for the bottom panels.

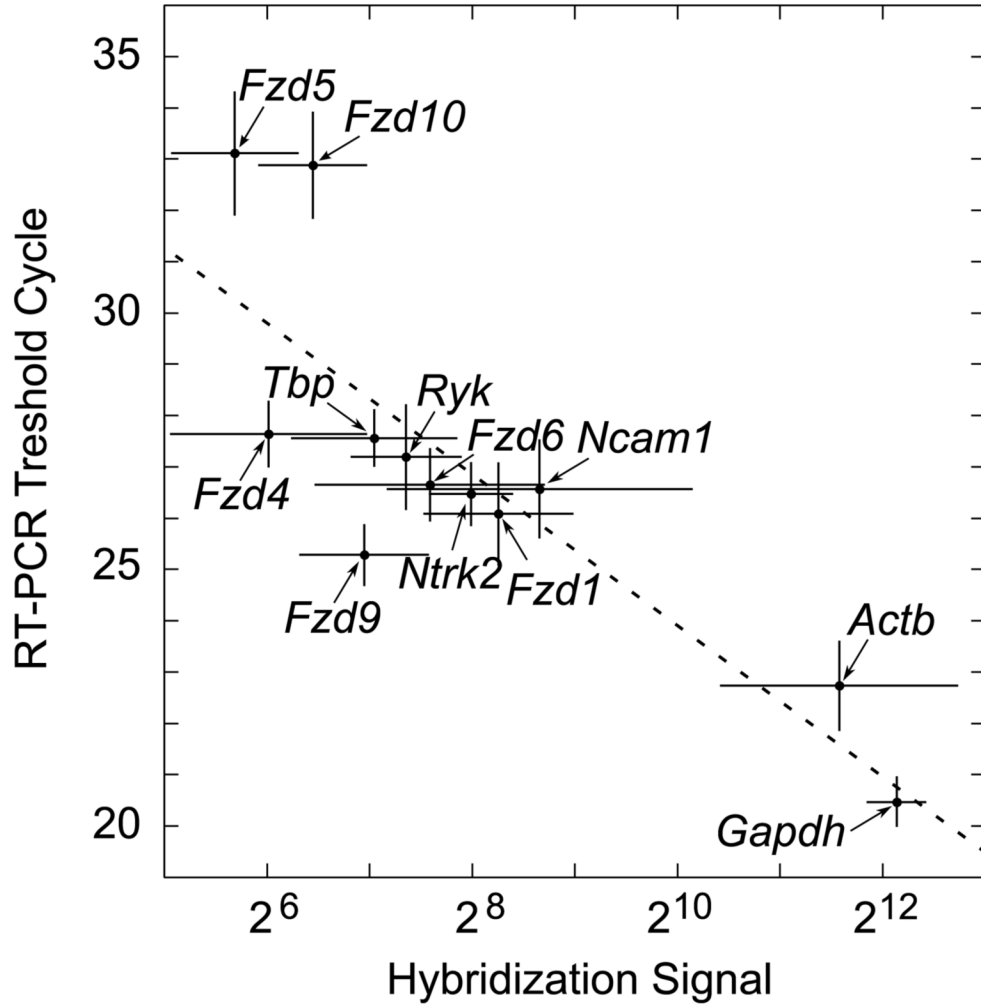


Fig. 5. Correlation of microarray and real-time RT-PCR analyses of Wnt-receptor expression within the cochlea

The hybridization signals are from the meta-analysis of our microarray data and those of Someya and colleagues (Table 2 and Supplement Table 1). The RT-PCR threshold cycles are the means from the modioli of twelve separate, nine-week-old animals. The Pearson's coefficient for the fitted straight line equaled -0.84 , indicating a significant correlation ($P < 0.001$). Error bars, standard deviations; gene symbols, see Table 1.

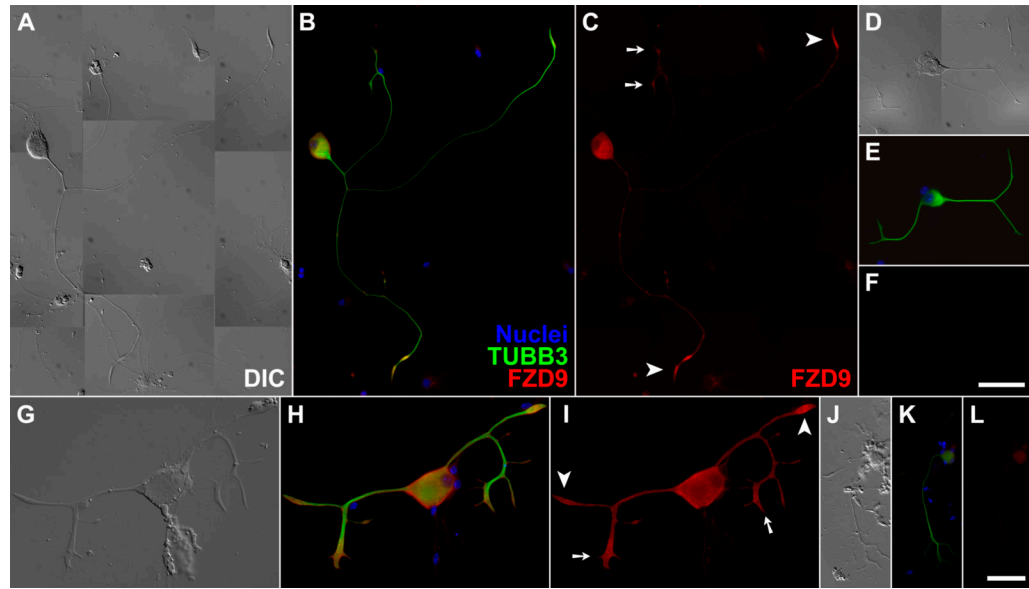


Fig. 6. FZD9 protein localized to growth cones of regenerating adult spiral ganglion neurons in primary culture

(A/D/G/J) Differential interference contrast (DIC); (B/E/H/K) three-channel epifluorescence with nuclei colored in blue, the neuronal marker β III-tubulin in green (TUBB3), and FZD9 in red; (C/F/I/L) red-channel fluorescence alone. Only weak background labeling was observed in non-neuronal cells, or when the FZD9 antibodies were omitted (D–F) or replaced by normal rabbit IgG (J–L). Arrowheads, “simple” growth cones; arrows, “complex” growth cones; scalebar in F for panels A–F, 50 μ m; scalebar in L for panels G–I and J–L, 17.5 and 30 μ m, respectively. The samples in A–F were processed and imaged under identical conditions, as were those in G–L.

Table 1
Oligonucleotide primers

| Gene Symbol ^a | Primer Pair (5' to 3') | Product Size (bp) |
|---|--|-------------------|
| <i>For qualitative and real-time RT-PCR</i> | | |
| <i>Actb</i> | GGCTGTATTCCCCTCCATCG CCAGTTGGTAACAATGCCATGT | 154 |
| <i>Fzd1</i> | GCGACGTACTGAGCGGAGTG TGATGGTGCGGATGCGGAAG | 150 |
| <i>Fzd2</i> | CTCAAGGTGCCGTCTATCTCAG GCAGCACAAACCCGACCATG | 156 |
| <i>Fzd3</i> | GGTGTCCCGTGGCCTGAAG ACGTGCAGAAAGGAATAGCCAAG | 194 |
| <i>Fzd4</i> | GACAACTTTCACGCCGCTCATC CCAGGCAAACCCAAATTCTCTCAG | 181 |
| <i>Fzd5</i> | AAGCTGCCTTCGGATGACTA TGCACAAGTTGCTGAACTCC | 129 |
| <i>Fzd6</i> | TGTTGGTATCTCTGCGGTCTTCTG CTCGGCGGCTTCACTGATG | 110 |
| <i>Fzd7</i> | ATATCGCCTACAACCAGACCATCC AAGGAACGGCACGGAGGAATG | 193 |
| <i>Fzd8</i> | GTTTCAGTCATCAAGCAGCAAGGAG AAGGCAGGCGACAACGACG | 122 |
| <i>Fzd9</i> | ATGAAGACGGGAGGCACCAATAC TAGCAGACAATGACGCAGGTGG | 107 |
| <i>Fzd10</i> | ATCGGCACTTCCTTCATCCTGTG TCTTCCAGTAGTCCATGTTGAG | 199 |
| <i>Gapdh</i> | CCCCAATGTGTCCGTCGTG GCCTGCTTACCACCTTCT | 84 |
| <i>Ncam1</i> | CCCAGCCAAGGAGAAATCAG CTGGTTTGGGCTCAGCTTCT | 123 |
| <i>Ntrk2</i> | CTGGGGCTTATGCCTGCTG AGGCTCAGTACACCAAATCCTA | 100 |
| <i>Ryk</i> | GGTCTTGATGCAGAGCTTTACT CCCATAGCCACAAAGTTGTCTAC | 170 |
| <i>Tbp</i> | CCCCAACTCTTCCATTCT GCAGGAGTGATAGGGGTCAT | 103 |
| <i>For cloning partial cDNAs as riboprobe templates</i> | | |
| <i>Fzd1</i> | CAGGTTCTGCAAAAGCTTCC TCGGTTACTGCACTCCCTCT | 682 |
| <i>Fzd2</i> | TTTAAAAGCTGCCCTGTGCT CTACCGGAGAGAAGGGAAC | 642 |
| <i>Fzd3</i> | TTTGGGTTGGAAGCAAAAAG GAACTCTGCCCAAGAAAGC | 616 |
| <i>Fzd4</i> | AATTCTAGGCAGCCCTGTT | 658 |

| Gene Symbol ^a | Primer Pair (5' to 3') | Product Size (bp) |
|--------------------------|---|-------------------|
| <i>Fzd5</i> | CCAGCATTCTGGAGGTTTCAT CACTCAAGACTCCGGAGAGG TCCTGGGAGTGTAGGTTTGG | 607 |
| <i>Fzd6</i> | TTGCTAGCCCTGACTGTCCT CTCCTTTTGGGGAAGGTAGG | 613 |
| <i>Fzd7</i> | TTTCAAGAGGAGGCCAAGAA CCCTGTCTGGAGGAAAAACA | 609 |
| <i>Fzd8</i> | TGGCAGGACATGAGAAAAGTG CGGTTGTGCTGCTCATAGAA | 682 |
| <i>Fzd9</i> | AGTTTCCTCCTGACCGGTTT CAAGGCCCTGAGCTTTACTG | 692 |
| <i>Fzd10</i> | CTTTGCTGCCTGTGCATAAA CAATAAGCCCTCTGGTGCTC | 616 |
| <i>Ryk</i> | GAACGACTTGCGAAGTGTC CAGAGTCATGAGCTCCACA | 700 |

^a *Actb*, actin, beta; *Gapdh*, glyceraldehyde-3-phosphate dehydrogenase; *Ncam1*, neural cell adhesion molecule 1; *Ntrk2*, neurotrophic tyrosine kinase, receptor, type 2; *Tbp*, TATA box binding protein.

* Significantly above 44th-percentile cutoff of 5.10 in one-sided *t* tests with 1,369 probe sets for neuronal transmembrane receptors ($P < 0.05$ after Bonferroni correction).